AIAA JOURNAL
Vol. 47, No. 5, May 2009

Direct Quadrature Method of Moments Solution of Fokker–Planck Equations in Aeroelasticity

Peter J. Attar* and Prakash Vedula†
University of Oklahoma, Norman, Oklahoma 73019

DOI: 10.2514/1.40292

The direct quadrature method of moments is presented as an efficient and accurate means of numerically computing solutions of the Fokker–Planck equation. The theoretical details of the solution procedure are first presented. The method is then used to solve the Fokker–Planck equations for both one- and two-dimensional processes that possess nonlinear stochastic differential equations. Higher-order moments of the stationary solutions are computed and prove to be very accurate when compared with analytic (one-dimensional process) and Monte Carlo (two-dimensional process) solutions. Trends in the standard deviation and coefficient of kurtosis with respect to the additive noise level and bifurcation parameter are reported for what appears to be the first time for the saddle-node/subcritical Hopf bifucation problem. The deterministic form of this problem exhibits hysteresis, which is often a phenomenon present in more-complex nonlinear aeroelastic systems. Finally, statistical results are shown for a typical section airfoil with nonlinear stiffness subjected to random aerodynamic loading. The constants for the nonlinear stiffness are chosen such that the deterministic behavior exhibits both a saddle-node and subcritcal bifurcation. Standard deviation results computed using the direct quadrature method of moments for a reduced frequency below the deterministic saddle-node bifurcation point compare well with Monte Carlo results.

Nomenclature

$\bar{h}$	=	normalized plunge degree of freedom, h/b
b	=	reference airfoil length
e	=	distance from aerodynamic center to elastic axis
K_h	=	constant for linear plunge stiffness term
K_h^{nl}	=	constant for cubic plunge stiffness term
K_α	=	constant for linear pitch stiffness term
K_α^{nl1}	=	constant for cubic pitch stiffness term
K_α^{nl2}	=	constant for quintic pitch stiffness term
k	=	reduced frequency, $\frac{\omega_\alpha b}{U}$
m	=	airfoil mass per unit length
r_α	=	radius of gyration
S_α	=	mass unbalance
U	=	freestream flow velocity
x_α	=	S_α/mb
y	=	$\bar{h}'$
z	=	α'
α	=	pitch degree of freedom
ξ_h	=	plunge mode damping ratio
ξ_α	=	pitch mode damping ratio
τ	=	nondimensional time, $t\omega_\alpha$
ω_h	=	plunge uncoupled natural frequency
ω_α	=	pitch uncoupled natural frequency
$'$	=	$\frac{\mathrm{d}}{\mathrm{d}\tau}$

Presented as Paper 1986 at the 49th AIAA/ASME/ASCE/AHS/ASC Structures, Structural Dynamics, and Materials Conference 16th AIAA/ASME/AHS Adaptive Structures Conference 10th AIAA Non-Deterministic Approaches Conference 9th AIAA Gossamer Spacecraft Forum 4th AIAA Multidisciplinary Design Optimization Specialist Conference, Schaumburg, IL, 7–10 April 2008; received 6 August 2008; revision received 6 January 2009; accepted for publication 8 February 2009.

*Assistant Professor, Department of Aerospace and Mechanical Engineering, 865 Asp Avenue, Felgar Hall; peter.attar@ou.edu. Member AIAA.

†Assistant Professor, Department of Aerospace and Mechanical Engineering, 865 Asp Avenue, Felgar Hall; pvedula@ou.edu.

I. Introduction

CHARACTERIZATION of the response of stochastic systems is of interest for engineers in many different disciplines. This is particularly true in the field of structural dynamics, in which loads and various system parameters can often be thought of as random processes. For example, in the field of aeroelasticity, Ibrahim et al. considered the pressure fluctuations due to a turbulent boundary layer as random forces when analyzing panel flutter [1–3]. Vaicaitis et al. [4] and Olson [5] also considered this problem and used Monte Carlo simulations. Recently, much work has been done in the area of parametric uncertainty quantification for aeroelastic problems. For a nice overview of some of this work and the remaining challenges, see the work of Pettit [6].

The response of a structural dynamic system to random excitation with delta correlation can be considered a Markovian process. Furthermore, even if a process is non-Markovian, by introducing additional random variables, one can get a Markovian process [7]. The transition probability density for a Markovian process is governed by an appropriate Fokker–Planck (FP) equation. Exact solutions of the FP equation are known for only a few systems. In most cases, approximate solutions need to be found using either analytic or numerical methods. Risken [7] presented many such analytical methods. Examples of approximate analytical solutions are the van Kampen expansion method [8,9], the method of matrix continued fractions [10], and path integral solutions [11]. In terms of numerical methods, finite difference and finite element methods appear to be the most popular [12–15]. Although these methods can give accurate solutions, the computational expense can be prohibitive for Fokker–Planck equations with dimensions larger than 2.

In this paper, we present an efficient and accurate method for the solution of the Fokker–Planck equations for stochastic processes. This method is based upon the direct quadrature method of moments (DQMOM), first introduced by Fox et al. [16–18] for the numerical solution of the population balance equations for multiphase flow predictions. Recently, this method has also been used to compute numerical solutions for the Boltzmann equation by Vedula and Fox [19] and for one- and two-dimensional Fokker–Planck equations arising in nonlinear dynamics [20]. Here we will show additional results for a two-dimensional Fokker–Planck equation that corresponds to a deterministic system that has both a saddle-node bifurcation and a subcritical Hopf bifurcation. Knowledge of the

statistical moment behavior of such a system is important due to its similarity to more complex nonlinear aeroelastic systems. Finally, results will be presented for such an aeroelastic system: a typical section airfoil with 2 degrees of freedom (pitch and plunge). A nonlinear structural model in the form of nonlinear springs in the pitch and plunge degrees of freedom is presented for this model. This dynamical system results in a four-dimensional Fokker–Planck equation.

II. Theory

An abbreviated discussion of the Fokker–Planck equation is given here. For a more detailed discussion of this equation, please see [7,21].

Given the set of stochastic differential equations in N variables $\mathbf{x} = \{x_1, x_2, \ldots, x_N\}$,

$$\dot{x}_i = h_i(\mathbf{x}, t) + g_{ij}(\mathbf{x}, t)\Gamma_j(t) \tag{1}$$

where the $\Gamma_j(t)$ are Gaussian random variables with the following correlations:

$$\langle \Gamma_i(t) \rangle = 0 \qquad \langle \Gamma_i(t)\Gamma_j(t') \rangle = 2\delta_{ij}\delta(t - t') \tag{2}$$

where δ_{ij} is the Kronecker delta, and $\delta(t - t')$ is the delta function; a Fokker–Planck equation for the transition probability $P(\mathbf{x}, t|\mathbf{x}', t')$ can be written in the following form:

$$\frac{\partial P(\mathbf{x}, t|\mathbf{x}', t')}{\partial t} = -\frac{\partial}{\partial x_i}\left[D_i^{(1)}(\mathbf{x}, t)P(\mathbf{x}, t|\mathbf{x}', t')\right] + \frac{\partial^2}{\partial x_i \partial x_j}\left[D_{ij}^{(2)}(\mathbf{x}, t)P(\mathbf{x}, t|\mathbf{x}', t')\right] \tag{3}$$

It can also be shown that the probability density function, $f(\mathbf{x}, t)$, also satisfies the Fokker–Planck equation:

$$\frac{\partial f(\mathbf{x}, t)}{\partial t} = -\frac{\partial}{\partial x_i}\left[D_i^{(1)}(\mathbf{x}, t)f(\mathbf{x}, t)\right] + \frac{\partial^2}{\partial x_i \partial x_j}\left[D_{ij}^{(2)}(\mathbf{x}, t)f(\mathbf{x}, t)\right] \tag{4}$$

In Eqs. (3) and (4), the drift ($D_i^{(1)}(\mathbf{x}, t)$) and diffusion ($D_{ij}^{(2)}(\mathbf{x}, t)$) coefficients are defined as [using the notation of Eq. (1)]:

$$D_i^{(1)}(\mathbf{x}, t) = h_i(\mathbf{x}, t) \tag{5}$$

$$D_{ij}^{(2)}(\mathbf{x}, t) = g_{ik}(\mathbf{x}, t)g_{jk}(\mathbf{x}, t) \tag{6}$$

and are derived using the Itô calculus [7]. Note in Eqs. (3) and (4) that summation notation is assumed.

To simplify the derivations, Eq. (4) will be specialized to the problem of $N = 2$ and all cross diffusion terms will be assumed to be zero ($D_{12}^{(2)} = D_{21}^{(2)} = 0$). Also, $D_{11}^{(2)}$ will be assumed to be zero. In practice, generalizing the method (to be discussed in this paper) to higher dimensions with all terms included does not complicate the computational procedure. With the aforementioned simplifications, we get the following for the Fokker–Planck equations:

$$\frac{\partial f(\mathbf{x}, t)}{\partial t} = -\frac{\partial}{\partial x}\left[D_1^{(1)} f(\mathbf{x}, t)\right] - \frac{\partial}{\partial y}\left[D_2^{(1)} f(\mathbf{x}, t)\right] + \frac{\partial^2}{\partial y^2}\left(D_{22}^{(2)} f(\mathbf{x}, t)\right) \tag{7}$$

where now $\mathbf{x} = \{x, y\}^T$.

In the direct quadrature method of moments approach, the probability density is written as a weighted summation of the products of the Dirac delta functions:

$$f(\mathbf{x}, t) = \sum_{i=1}^{M} w_i(t)\delta(x - x_i(t))\delta(y - y_i(t)) \tag{8}$$

where M is the number of delta functions (compute nodes), and $w_i(t)$, $x_i(t)$, and $y_i(t)$ are the dependent variables for compute node i.

In the rest of the paper, w_i will be called weights and x_i and y_i the abscissas. Also, the explicit expression of the dependent variables as functions of time will be dropped to condense the notation. If the delta functions $\delta(x - x_i)$ and $\delta(y - y_i)$ are written as $\delta_i^{(x)}$ and $\delta_i^{(y)}$, respectively, substitution of Eq. (8) into Eq. (7) results in the following:

$$\sum_{i=1}^{M}\left[\frac{\partial w_i}{\partial t}\delta_i^{(x)}\delta_i^{(y)} - w_i\frac{\partial x_i}{\partial t}\frac{\partial \delta_i^{(x)}}{\partial x}\delta_i^{(y)} - w_i\frac{\partial y_i}{\partial t}\delta_i^{(x)}\frac{\partial \delta_i^{(y)}}{\partial y}\right] = \sum_{i=1}^{M}\left[-\frac{\partial}{\partial x}\left(D_1^{(1)}w_i\delta_i^{(x)}\delta_i^{(y)}\right) - \frac{\partial}{\partial y}\left(D_2^{(1)}w_i\delta_i^{(x)}\delta_i^{(y)}\right) + \frac{\partial^2}{\partial y^2}\left(D_{22}^{(2)}w_i\delta_i^{(x)}\delta_i^{(y)}\right)\right] \tag{9}$$

Defining new variables, which we will call the weighted abscissas, $\mu_i^{(x)} = w_i x_i$ and $\mu_i^{(y)} = w_i y_i$, Eq. (9) becomes

$$\sum_{i=1}^{M}\left[\frac{\partial w_i}{\partial t}\delta_i^{(x)}\delta_i^{(y)} - \frac{\partial \mu_i^{(x)}}{\partial t}\frac{\partial \delta_i^{(x)}}{\partial x}\delta_i^{(y)} + x_i\frac{\partial w_i}{\partial t}\frac{\partial \delta_i^{(x)}}{\partial x}\delta_i^{(y)} - \frac{\partial \mu_i^{(y)}}{\partial t}\frac{\partial \delta_i^{(y)}}{\partial y}\delta_i^{(x)} + y_i\frac{\partial w_i}{\partial t}\frac{\partial \delta_i^{(y)}}{\partial y}\delta_i^{(x)}\right] = \sum_{i=1}^{M}\left[-\frac{\partial}{\partial x}\left(D_1^{(1)}w_i\delta_i^{(x)}\delta_i^{(y)}\right) - \frac{\partial}{\partial y}\left(D_2^{(1)}w_i\delta_i^{(x)}\delta_i^{(y)}\right) + \frac{\partial^2}{\partial y^2}\left(D_{22}^{(2)}w_i\delta_i^{(x)}\delta_i^{(y)}\right)\right] \tag{10}$$

At this point, we have one equation in $3M$ unknowns. To close this equation, we will take $3M$ moments of it. Recalling that the generalized moment $\langle x^r y^s \rangle$ for nonnegative integers r and s is given by the following expression:

$$\langle x^r y^s \rangle = \int_{-\infty}^{\infty} x^r y^s f(x, y, t)\,\mathrm{d}x\,\mathrm{d}y \tag{11}$$

the evolution of $\langle x^r y^s \rangle$ can be obtained by taking the moment of Eq. (10) (after interchanging the order of summation and integration and combining the sums on the left- and right-hand sides):

$$\sum_{i=1}^{M}\left[\int_{-\infty}^{\infty}\int_{-\infty}^{\infty} x^r y^s\left[\frac{\partial w_i}{\partial t}\delta_i^{(x)}\delta_i^{(y)} - \frac{\partial \mu_i^{(x)}}{\partial t}\frac{\partial \delta_i^{(x)}}{\partial x}\delta_i^{(y)} + x_i\frac{\partial w_i}{\partial t}\frac{\partial \delta_i^{(x)}}{\partial x}\delta_i^{(y)} - \frac{\partial \mu_i^{(y)}}{\partial t}\frac{\partial \delta_i^{(y)}}{\partial y}\delta_i^{(x)} + y_i\frac{\partial w_i}{\partial t}\frac{\partial \delta_i^{(y)}}{\partial y}\delta_i^{(x)}\right]\mathrm{d}x\mathrm{d}y\right] = \sum_{i=1}^{M}\left[\int_{-\infty}^{\infty}\int_{-\infty}^{\infty} x^r y^s\left[-\frac{\partial}{\partial x}\left(D_1^{(1)}w_i\delta_i^{(x)}\delta_i^{(y)}\right) - \frac{\partial}{\partial y}\left(D_2^{(1)}w_i\delta_i^{(x)}\delta_i^{(y)}\right) + \frac{\partial^2}{\partial y^2}\left(D_{22}^{(2)}w_i\delta_i^{(x)}\delta_i^{(y)}\right)\right]\mathrm{d}x\mathrm{d}y\right] \tag{12}$$

In simplifying Eq. (12), the following properties of the Dirac delta function are used:

$$\int x^r\delta(x - x_i)\,\mathrm{d}x = x_i^r \tag{13}$$

$$\int x^r\frac{\mathrm{d}\delta(x - x_i)}{\mathrm{d}x}\,\mathrm{d}x = -rx_i^{r-1} \tag{14}$$

Therefore, by using Eqs. (13) and (14) and integrating by parts the right-hand side of Eq. (12), we get the following equation:

$$\sum_{i=1}^{M}\Bigg[x_i^r y_i^s \frac{\partial w_i}{\partial t} + r x_i^{r-1} y_i^s \frac{\partial \mu_i^{(x)}}{\partial t} - r x_i^{r-1} y_i^s x_i \frac{\partial w_i}{\partial t} + s x_i^r y_i^{s-1} \frac{\partial \mu_i^{(y)}}{\partial t} - s x_i^r y_i^{s-1} y_i \frac{\partial w_i}{\partial t}\Bigg]$$
$$= \sum_{i=1}^{M}\Bigg[-x^r y^s D_1^{(1)} w_i \delta_i^{(x)} \delta_i^{(y)}|_{-\infty}^{\infty} + r x_i^{r-1} y_i^s D_1^{(1)}|_{x_i,y_i} w_i - x^r y^s D_2^{(1)} w_i \delta_i^{(x)} \delta_i^{(y)}|_{-\infty}^{\infty} + s x_i^r y_i^{s-1} D_2^{(1)}|_{x_i,y_i} w_i + x^r y^s \frac{\partial}{\partial y}\left(D_{22}^{(2)} w_i \delta_i^{(x)} \delta_i^{(y)}\right)|_{-\infty}^{\infty} - s x^r y^{s-1} D_{22}^{(2)} w_i \delta_i^{(x)} \delta_i^{(y)}|_{-\infty}^{\infty} + s(s-1) x_i^r y_i^{s-2} D_{22}^{(2)}|_{x_i,y_i}\Bigg] \quad (15)$$

where $|_{x_i,y_i}$ denotes the evaluation of the drift and diffusion terms at $x = x_i$ and $y = y_i$. Using the property that the probability density and its derivatives vanish at positive and negative infinity and the assumption of boundedness (and continuity) of moments, the boundary terms in Eq. (15) vanish, leaving the following equation after simplification:

$$\sum_{i=1}^{M}\Bigg[[1-(r+s)] x_i^r y_i^s \frac{\mathrm{d}w_i}{\mathrm{d}t} + r x_i^{r-1} y_i^s \frac{\mathrm{d}\mu_i^{(1)}}{\mathrm{d}t} + s x_i^r y_i^{s-1} \frac{\mathrm{d}\mu_i^{(2)}}{\mathrm{d}t}\Bigg]$$
$$= \sum_{i=1}^{M}[r x_i^{r-1} y_i^s D_1^{(1)}|_{x_i,y_i} w_i + s x_i^r y_i^{s-1} D_2^{(1)}|_{x_i,y_i} w_i + s(s-1) x_i^r y_i^{s-2} D_{22}^{(2)}|_{x_i,y_i} w_i] \quad (16)$$

This is now a nonlinear differential equation for each of the weights and weighted abscissas. There are $3M$ such equations, which in matrix form can be written as follows:

$$\mathbf{A}\mathbf{z} = \mathbf{F}(\mathbf{w}, \mathbf{x}, \mathbf{y}) \quad (17)$$

where the matrix $\mathbf{A}$ is a nonlinear function of the abscissas and $\mathbf{z} = \{\frac{\mathrm{d}\mathbf{w}}{\mathrm{d}t}, \frac{\mathrm{d}\boldsymbol{\mu}^{(1)}}{\mathrm{d}t}, \frac{\mathrm{d}\boldsymbol{\mu}^{(2)}}{\mathrm{d}t}\}^T$. Also, $\mathbf{w}$, $\mathbf{x}$, $\mathbf{y}$, and $\boldsymbol{\mu}$ are the vectors of weights, abscissas, and weighted abscissas, respectively. Equation (17) is a set of implicit nonlinear ordinary differential equations. To solve these equations, the DDASPK software package [22–24] is used. An example of this system of equations is given in the Appendix for the nonlinear one-dimensional system presented in Sec. III.A.

It may be noted that the selection of constraints on low-order moments should also ensure that the condition number of matrix $\mathbf{A}$ in Eq. (17) is relatively small (compared with the multiplicative inverse of machine precision). Although these criteria may not lead to a unique selection of moments, we based our moment constraint selection procedure on including all low-order moments (up to a certain order) followed by the successive elimination of constraints that would result in an ill-conditioned system. In this paper, we also ensure that the final moment constraint selection gives results that have satisfactory agreement with those obtained from complementary methods (e.g., analytical and/or Monte Carlo methods). The particular choice of moment constraints can be problem dependent due to the quadrature-based closure approximation used to model the unclosed moments. Although we expect convergence (not necessarily uniform) with an increase in the number of moment constraints and quadrature points, the convergence rates are also problem dependent for general nonlinear systems.

III. Example Problems

Four example problems will be given in this paper to demonstrate the effectiveness of the DQMOM method in solving the Fokker–Planck equation. The problems will be presented in order of increasing difficulty.

A. One-Dimensional Nonlinear Process

The first problem is the nonlinear process with a stochastic ordinary differential equation given by

$$dX = (X - X^3)dt + \sigma dW \quad (18)$$

which has the Fokker–Planck equation given by

$$\frac{\partial f}{\partial t} = -\frac{\partial}{\partial x}\left[(x - x^3) f\right] + \frac{\sigma^2}{2}\frac{\partial^2 f}{\partial x^2} \quad (19)$$

The deterministic counterpart to this equation ($\mathrm{d}x/\mathrm{d}t = x - x^3$) has two asymptotically stable equilibrium points, $x = \pm 1$, separated by an unstable equilibrium point at $x = 0$. An analytical solution to Eq. (19) is not known but the stationary solution is given by

$$P(x) = c e^{(x^2 - 0.5x^4)/\sigma^2} \quad (20)$$

where c is a normalization constant and is computed such that the integral of Eq. (20) is equal to 1. Figures 1–3 show the second, fourth, and sixth moments as computed by the DQMOM numerical method as a function of the noise level σ. Also shown in these figures are the analytical results computed via Eq. (20). With only eight quadrature nodes, the DQMOM and analytical solutions agree quite well for each of the moments. Also note that all odd moments are zero for this problem and the DQMOM method computes these correctly as well.

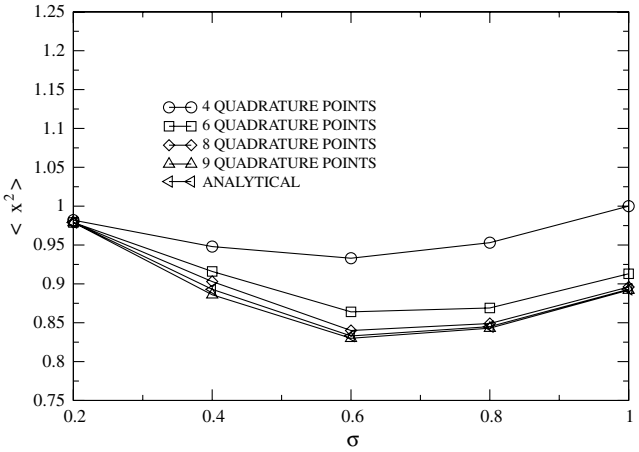

Fig. 1 One-dimensional FP equation; second moment of x vs the noise intensity level σ.

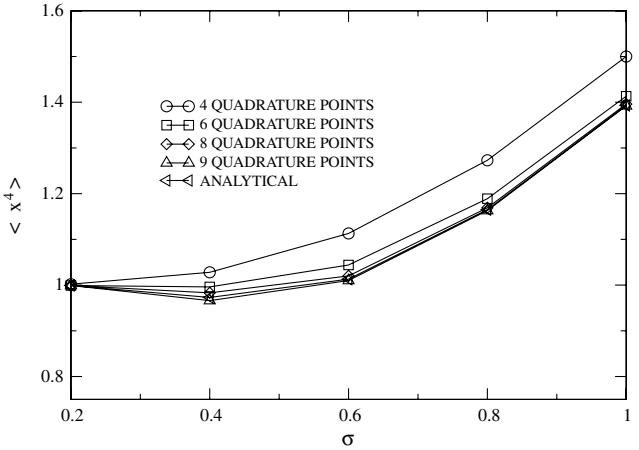

Fig. 2 One-dimensional FP equation; fourth moment of x vs the noise intensity level σ.

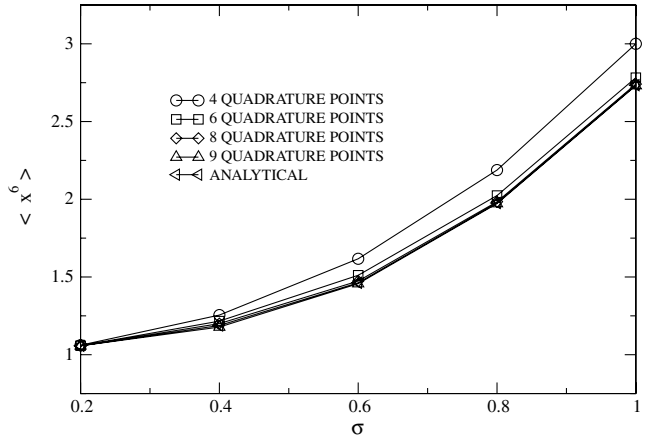

Fig. 3 One-dimensional FP equation; sixth moment of x vs the noise intensity level σ.

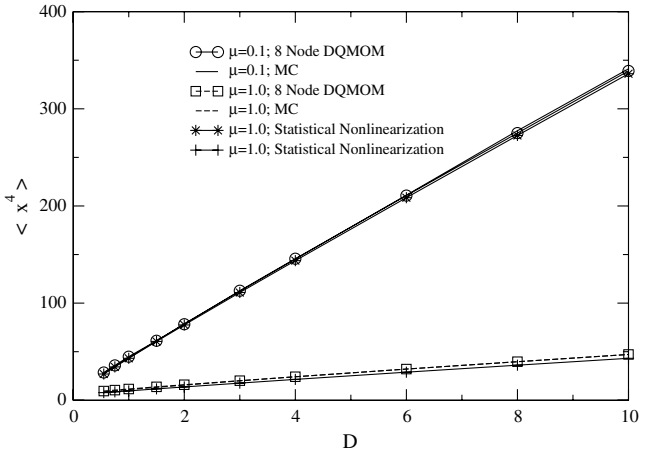

Fig. 5 FP for the van der Pol equation; fourth moment of x vs the noise intensity level D.

B. Two-Dimensional Van Der Pol Oscillator

The second problem that is investigated is the van der Pol oscillator subjected to stationary Gaussian white noise. If the vector process $\mathbf{Z}(t) = \{x(t), y(t)\}^T$ is introduced, where $y(t) = \dot{x}(t)$, the Itô-type stochastic differential equation can be written as follows:

$$d\mathbf{Z}(t) = \mathbf{f}(\mathbf{Z}(t))dt + \mathbf{Q}dW(t) \tag{21}$$

Here, we have

$$\mathbf{f}(\mathbf{Z}(t)) = \begin{Bmatrix} y(t) \\ -\mu[x(t)^2 - 1]y(t) - x(t) \end{Bmatrix} \tag{22}$$

$$\mathbf{Q} = \begin{Bmatrix} 0 \\ \sqrt{2D} \end{Bmatrix} \tag{23}$$

The corresponding Fokker–Planck equation for this problem can be written as follows:

$$\frac{\partial f}{\partial t} = \mu(x^2 - 1)f - y\frac{\partial f}{\partial x} + \Big[\mu(x^2 - 1)y + x\Big]\frac{\partial f}{\partial y} + D\frac{\partial^2 f}{\partial y^2} \tag{24}$$

which is solved numerically using the direct quadrature method of moments. The second and fourth moments of x as computed by a direct quadrature method of moments solution of Eq. (24) is shown in Figs. 4 and 5 for $\mu = 0.1$ and 1.0. Also shown in these figures is a numerical solution of the stochastic differential equation, Eq. (21), using a forward Euler–Maruyama time integration scheme. Because of its simplicity, we restricted our attention to the commonly used Euler–Maruyama scheme for integration of stochastic differential equations. It is plausible that high-order integration schemes for stochastic differential equations could lead to more accurate solutions with greater computational efficiency. The statistics from this solution were computed using a Monte Carlo solution with 5×10^5 particles and a time step of 0.0005 s. These figures also include moments computed using the stationary solutions from the analytic statistical nonlinearization procedure presented in [25]. In these figures, one can see that the second- and fourth-order moments computed using an eight-node direct quadrature method of moments solution compare favorably with the direct solution of the stochastic differential equation. Agreement with the statistical nonlinearization result is better for smaller values of the noise level D and the damping parameter μ, which is consistent with the approximations made with the analytic method. Note, to compute the direct quadrature method of moments solution, all moments up to the fifth order and $(r, s) = (6, 0)$, (5, 1), (4, 2) were taken [see Eq. (12)]. The direct quadrature method of moments solution is substantially faster than the direct solution of the stochastic differential equation. On an Intel T2500 2 GHz processor, 10 s of simulation time took 4 s of computational time using the direct quadrature method of moments solution and 1500 s of computational time using the Monte Carlo solution of the stochastic differential.

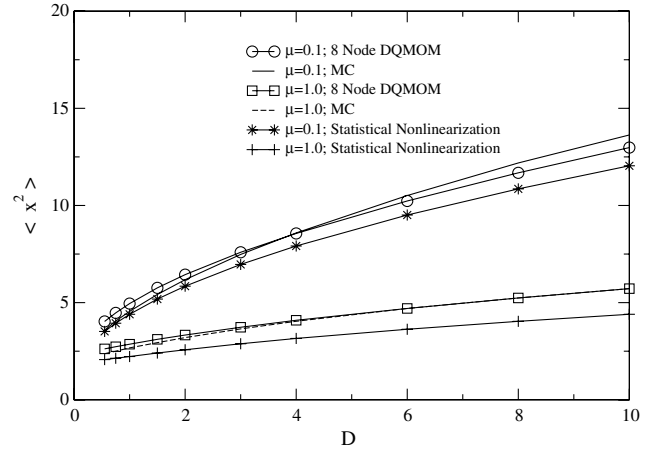

Fig. 4 FP for the van der Pol equation; second moment of x vs the noise intensity level D.

C. Two-Dimensional Nonlinear Process with Saddle-Node and Subcritical Bifurcation

The third problem that we will study is a stochastic version of the following nonlinear dynamical system in cylindrical coordinates [26]:

$$\dot{r} = \mu r + r^3 - r^5 \qquad \dot{\theta} = \omega + br^2 \tag{25}$$

Here, ω controls the frequency of infinitesimal oscillations and b determines the nonlinear dependency of the frequency on the oscillation amplitude. For $-1/4 < \mu < 0$, there are two attractors. One is a stable large-amplitude limit cycle oscillation (LCO) and the other is a stable attractor at the origin. At $\mu = -1/4$ the large amplitude LCO is destroyed via a saddle-node bifurcation and the only stable attractor is the origin. At $\mu = 0$, the system undergoes a subcritical Hopf bifurcation and the only attractor left is the large-amplitude limit cycle. This system exhibits a hysteretic behavior that is common in nonlinear aeroelastic systems [27] and presents a dangerous scenario that is often referred to as explosive flutter or "bad LCO." Traditional aeroelastic flutter tools are not able to predict the saddle-node bifurcation point, which results in an inability to predict where the actual dangerous region of the bifurcation parameter μ (Mach number, flow velocity, etc.) starts.

Equation (25) in Cartesian coordinates (x, y) is given by

$$\begin{aligned} \dot{x} &= \mu x + (1 - (x^2 + y^2))(x^2 + y^2)x - \omega y - b(x^2 + y^2)y \\ \dot{y} &= \mu y + (1 - (x^2 + y^2))(x^2 + y^2)y + \omega x + b(x^2 + y^2)x \end{aligned} \tag{26}$$

We will consider that the bifurcation parameter μ consists of a mean part μ_0 and a zero mean, Gaussian wideband random part $\mu_r(\tau)$, that is,

$$\mu = \mu_0 + \mu_r(\tau) \tag{27}$$

The Cartesian velocities $\dot{x}$ and $\dot{y}$ will also be subjected to uncorrelated, additive white noise terms $D_x(\tau)$ and $D_y(\tau)$. These additive noise terms will be considered uncorrelated with $\mu_r(\tau)$. Equations (26) can now be written as follows:

$$\begin{aligned}\dot{x} &= \mu_0 x + \mu_r(\tau)x + (1-(x^2+y^2))(x^2+y^2)x \\ &\quad - \omega y - b(x^2+y^2)y + D_x(\tau) \\ \dot{y} &= \mu_0 y + \mu_r(\tau)y + (1-(x^2+y^2))(x^2+y^2)y \\ &\quad + \omega x + b(x^2+y^2)x + D_y(\tau)\end{aligned} \tag{28}$$

The correlation functions for $\mu_r(\tau)$, $D_x(\tau)$, and $D_y(\tau)$ are given as follows:

$$C_{\mu\mu} = \langle \mu_r(\tau), \mu_r(\tau + d\tau)\rangle = 2D_m\delta(\Delta\tau) \tag{29}$$

$$C_{xx} = \langle D_x(\tau), D_x(\tau + d\tau)\rangle = 2D\delta(\Delta\tau) \tag{30}$$

$$C_{yy} = \langle D_y(\tau), D_y(\tau + d\tau)\rangle = 2D\delta(\Delta\tau) \tag{31}$$

where D_m and D are the spectral densities of the white noise processes $\mu_r(\tau)$ and $D_x(\tau)$ (and $D_y(\tau)$). Expressing the white noise processes as formal derivatives of the Brownian motion processes W_m, W_x, and W_y, the Itô-type stochastic differential equations, with the Wong–Zakai correction [28], corresponding to Eqs. (28) are given by

$$\begin{aligned}dx &= [\mu_0 x + (1-(x^2+y^2))(x^2+y^2)x - \omega y - b(x^2+y^2)y \\ &\quad + D_m x]d\tau + \sqrt{2D}dW_x(\tau) + \sqrt{2D_m}x dW_m(\tau)\end{aligned} \tag{32}$$

$$\begin{aligned}dy &= [\mu_0 y + (1-(x^2+y^2))(x^2+y^2)x + \omega x + b(x^2+y^2)x \\ &\quad + D_m y]d\tau + \sqrt{2D}dW_y(\tau) + \sqrt{2D_m}y dW_m(\tau)\end{aligned} \tag{33}$$

Finally, the Fokker–Planck equation that is to be numerically solved by the DQMOM method for this example is given by the following (including the Wong–Zakai correction):

$$\begin{aligned}\frac{\partial f}{\partial t} &= -\frac{\partial}{\partial x}[f(\mu_0 x + (1-(x^2+y^2))(x^2+y^2)x \\ &\quad - \omega y - b(x^2+y^2)y + D_m x)] \\ &\quad - \frac{\partial}{\partial y}[f(\mu_0 y + (1-(x^2+y^2))(x^2+y^2)y \\ &\quad + \omega x + b(x^2+y^2)x + D_m y)] + \frac{\partial^2}{\partial x^2}[f(D + D_m x^2)] \\ &\quad + 2\frac{\partial^2}{\partial x \partial y}[f(D_m xy)] + \frac{\partial^2}{\partial y^2}[f(D + D_m y^2)]\end{aligned} \tag{34}$$

Next, the stationary values of standard deviation and coefficient of kurtosis are presented for a DQMOM solution with 11 quadrature points and for a numerical solution of Eqs. (32) and (33) using a forward Euler–Maruyama time integration with a time step of 0.0002. The statistics reported for the numerical solution of Eqs. (32) and (33) are computed using a direct Monte Carlo simulation with 10,000 realizations. For the DQMOM solution, all moments up to the sixth order are closed along with the moments $[(r, s)]$: (5,2), (2,6), (2,5), (1,6), and (0,7). The values for ω and b are chosen as 1 and 0.01, respectively.

Figures 6–11 show the standard deviation and coefficient of kurtosis as a function of the additive noise level D. Statistics for three different values of the mean of the bifurcation parameter μ_0 are shown: $\mu_0 = -0.275$ (Figs. 6 and 7), which, for the deterministic system, is below the saddle-node value for μ_0; $\mu_0 = -0.100$ (Figs. 8 and 9), which is in the region where two attractors exist; and $\mu_0 = 0.100$ (Figs. 10 and 11), for which the only attractor is the large-amplitude LCO. In these figures, the level of multiplicative noise D_m (random coefficient component) is zero. Also shown in Figs. 8–11 are the corresponding values for the deterministic system, which exhibits a limit cycle at $\mu = -0.100$ and 0.100. First note that,

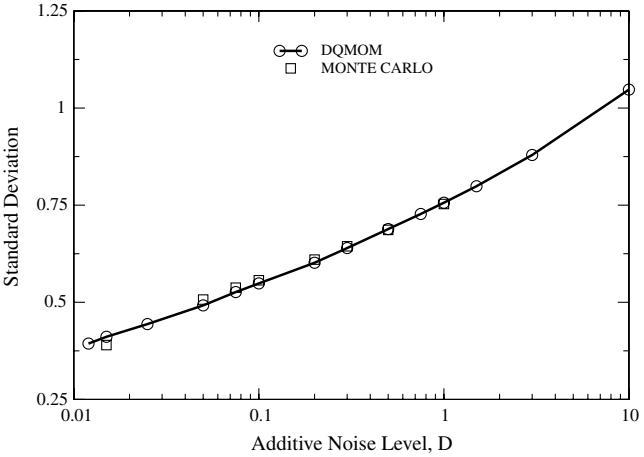

Fig. 6 Subcritical/saddle-node bifurcation example; standard deviation of x vs additive noise level D for $\mu_0 = -0.275$, $D_m = 0.0$.

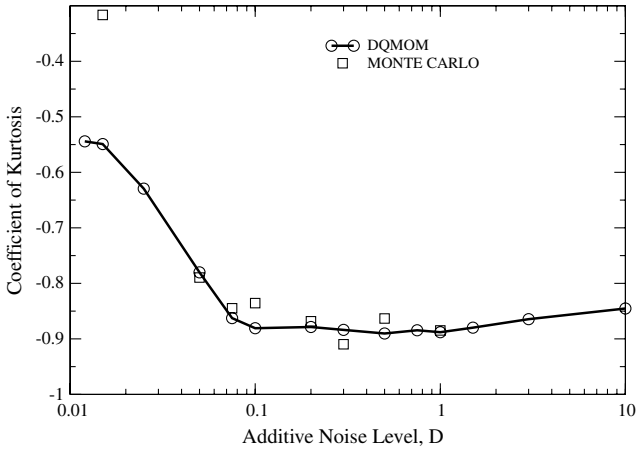

Fig. 7 Subcritical/saddle-node bifurcation example; coefficient of kurtosis of x vs additive noise level D for $\mu_0 = -0.275$, $D_m = 0.0$.

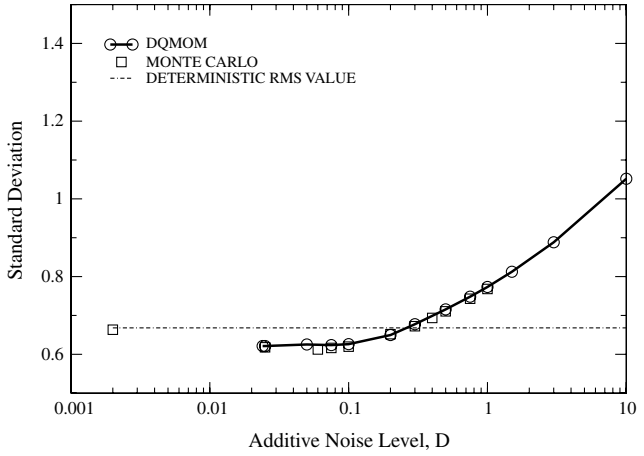

Fig. 8 Subcritical/saddle-node bifurcation example; standard deviation of x vs additive noise level D for $\mu_0 = -0.100$, $D_m = 0.0$.

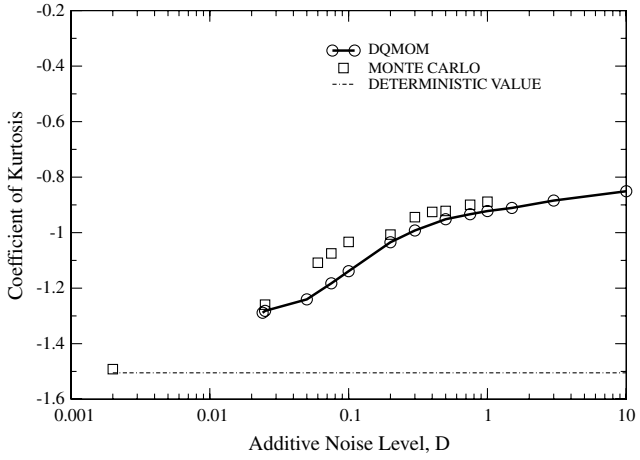

Fig. 9 Subcritical/saddle-node bifurcation example; coefficient of kurtosis of x vs additive noise level D for $\mu_0 = -0.100$, $D_m = 0.0$.

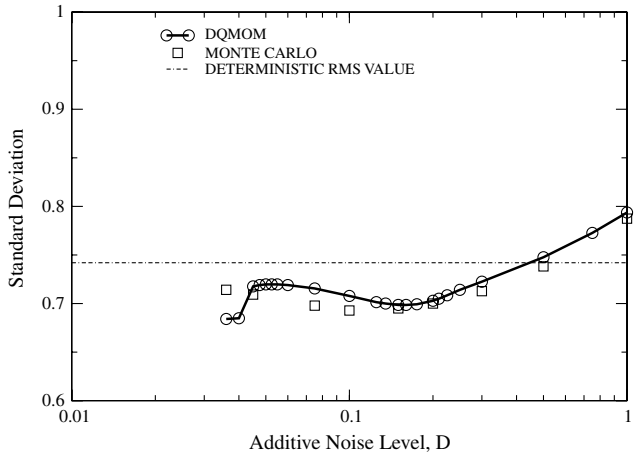

Fig. 10 Subcritical/saddle-node bifurcation example; standard deviation of x vs additive noise level D for $\mu_0 = 0.100$, $D_m = 0.0$.

in general, there is very good agreement between the DQMOM results and those from the numerical integration. As could be expected, the standard deviation results show better agreement. Two possible reasons for the differences in the kurtosis results are as follows:

1) If the evolution equations for the moments are written out, one will see that the equation that governs the evolution of the fourth moment ($\frac{\mathrm{d}}{\mathrm{d}t}\langle x^4\rangle$) will contain an eighth-order moment, $\langle x^8\rangle$, that is not closed in the current DQMOM solution with 11 quadrature points and closed moments as stated earlier.

2) A rigorous convergence study of the statistics computed with the Monte Carlo simulation has not been conducted with regard to the number of realizations and the time step.

Therefore, it is possible that the higher-order moments are not completely converged for the Monte Carlo results. Overall, however, the agreement is good and the qualitative trends match for both methods. For example, the kurtosis is sub-Gaussian (negative) for each value of μ_0. Whereas for $\mu_0 = -0.275$, the coefficient decreases with increasing additive noise level and appears to be approaching an asymptotic value, for $\mu_0 = -0.100$ and $\mu_0 = 0.100$, the coefficient of kurtosis increases with increasing additive noise level. For both values of μ_0, which correspond to cases in which a stable LCO exists, $\mu_0 = -0.100$ and 0.100, at low levels of noise the standard deviation versus the noise level curve is flat. This would seem to indicate that, for this level of additive noise, the system is mainly responding to the LCO with little influence from the noise. This is not the case for $\mu_0 = -0.275$, for which no LCO exists and the system is responding completely to the additive noise. Finally, it appears that for $\mu_0 = 0.100$, there is a local minimum in the standard deviation near $D = 0.15$, which is predicted by both the DQMOM and numerical integration methods. The DQMOM also predicts a local minimum of the coefficient of kurtosis near $D = 0.06$. This, however, is not predicted by the numerical integration.

Shown in Figs. 12–17 are the standard deviation and coefficient of kurtosis as a function of the ratio $\frac{2D_m}{\mu_0}$ for three different values of μ_0: -0.300, -0.100, and 0.100. The value of D for these figures is 0.10. Once again, the agreement between the DQMOM results and the numerical integration results are good. Overall, it appears that the standard deviation decreases with $2D_m/\mu_0$ but is not a strong function of this parameter, at least for the additive noise level used in these figures ($D = 0.100$). Also, the coefficient of kurtosis results are sub-Gaussian and decrease in magnitude as the ratio $2D_m/\mu_0$ increases. In particular, for $\mu_0 = -0.300$, which is below the saddle-node value for μ_0, the kurtosis seems to be approaching a switch from sub- to super-Gaussian behavior at or around $2D_m/\mu_0 = 1.5$.

D. Four-Dimensional Aeroelastic Typical Section Airfoil

The final example used to show the effectiveness of the DQMOM solution method is a dynamical system representing a typical section airfoil with pitch and plunge degrees of freedom in quasi-static subsonic flow [29]. The pitch and plunge stiffnesses are considered to be nonlinear with a cubic spring for the plunge degree of freedom and a cubic and quintic spring for the pitch degree of freedom. If the constant for the cubic term in the pitch degree of freedom is negative

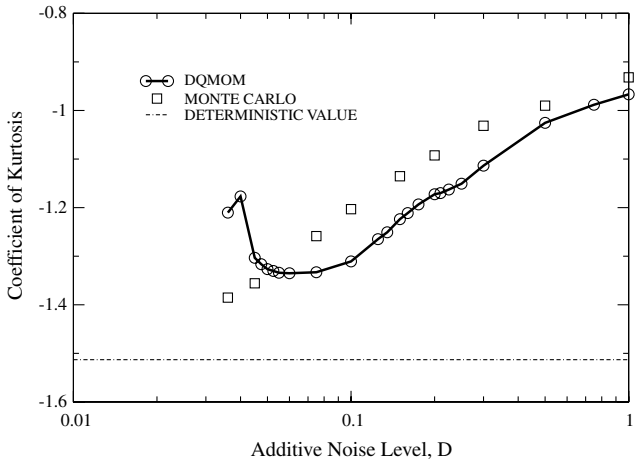

Fig. 11 Subcritical/saddle-node bifurcation example; coefficient of kurtosis of x vs additive noise level D for $\mu_0 = 0.100$, $D_m = 0.0$.

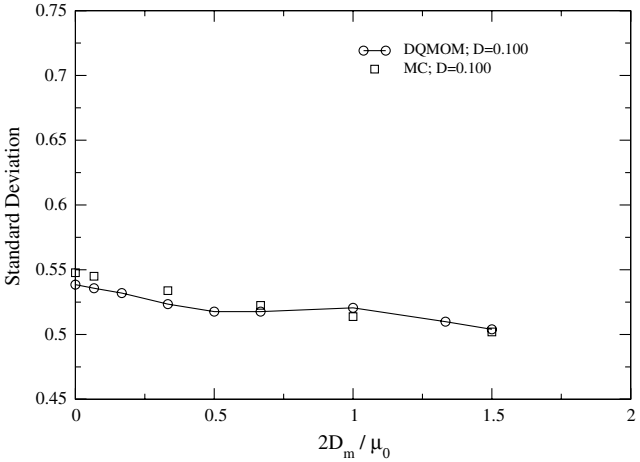

Fig. 12 Subcritical/saddle-node bifurcation example; standard deviation of x vs $2D_m/\mu_0$ for an additive noise level $D = 0.10$ and $\mu_0 = -0.300$.

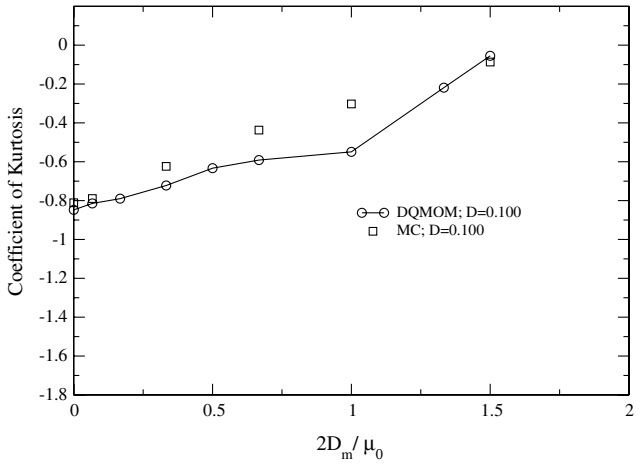

Fig. 13 Subcritical/saddle-node bifurcation example; coefficient of kurtosis of x vs $2D_m/\mu_0$ for an additive noise level $D = 0.10$ and $\mu_0 = -0.300$.

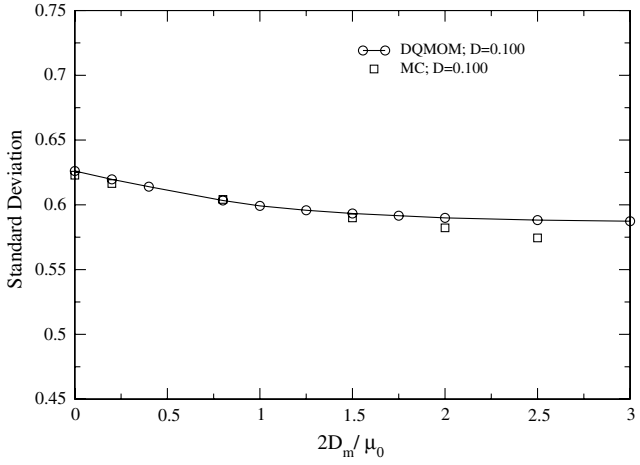

Fig. 14 Subcritical/saddle-node bifurcation example; standard deviation of x vs $2D_m/\mu_0$ for an additive noise level $D = 0.10$ and $\mu_0 = -0.100$.

and the quintic is considered positive, the deterministic system exhibits a subcritical Hopf bifurcation along with a saddle-node bifurcation, which results in hysteretic behavior. The dynamic system can be written as follows (after nondimensionalization):

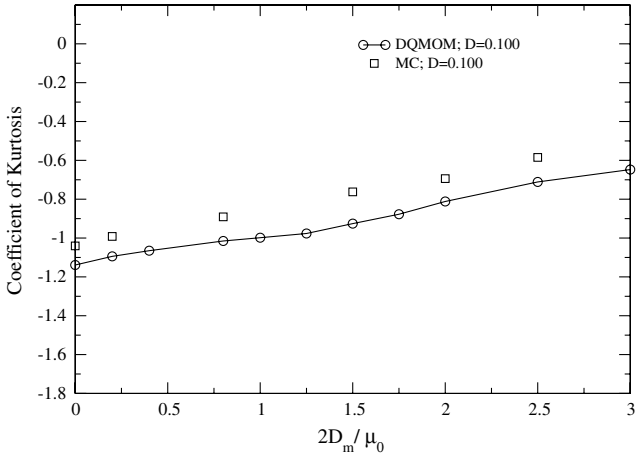

Fig. 15 Subcritical/saddle-node bifurcation example; coefficient of kurtosis of x vs $2D_m/\mu_0$ for an additive noise level $D = 0.10$ and $\mu_0 = -0.100$.

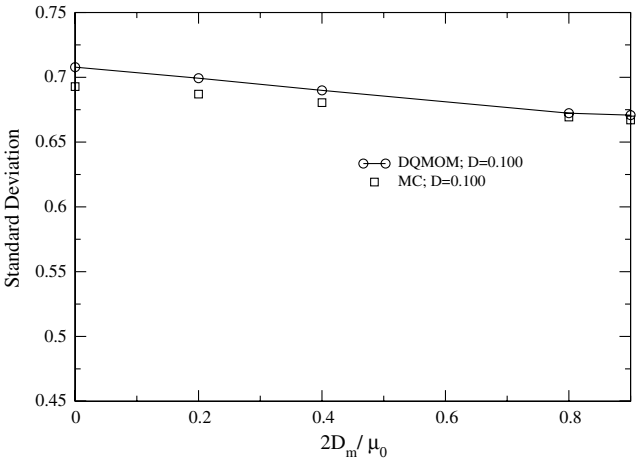

Fig. 16 Subcritical/saddle-node bifurcation example; standard deviation of x vs $2D_m/\mu_0$ for an additive noise level $D = 0.10$ and $\mu_0 = 0.100$.

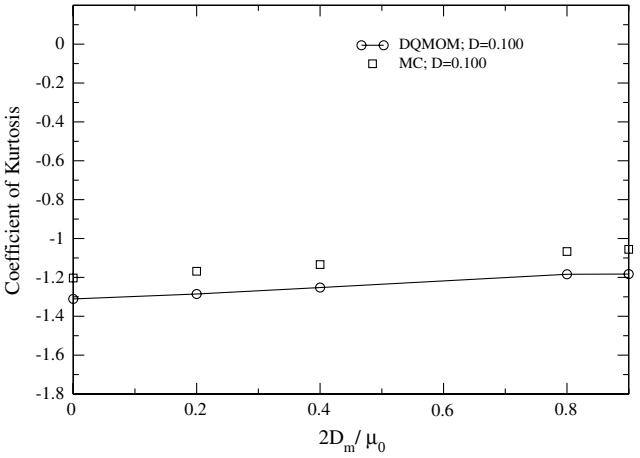

Fig. 17 Subcritical/saddle-node bifurcation example; coefficient of kurtosis of x vs $2D_m/\mu_0$ for an additive noise level $D = 0.10$ and $\mu_0 = 0.100$.

$$\bar{h}'' + x_\alpha \alpha'' + 2\xi_h \frac{\omega_h}{\omega_\alpha}\bar{h}' + \left(\frac{\omega_h}{\omega_\alpha}\right)^2 \left(\bar{h} + b^2 \frac{K_h^{nl}}{K_h}\bar{h}^3\right) = -\pi \frac{k}{\mu}(\bar{h}' + k\alpha) + L(\tau) \tag{35}$$

$$\alpha'' + \frac{x_\alpha}{r_\alpha^2}\bar{h}'' + 2\xi_\alpha \alpha' + \alpha + \frac{K_\alpha^{nl1}}{K_\alpha}\alpha^3 + \frac{K_\alpha^{nl2}}{K_\alpha}\alpha^5 = \pi \frac{e}{b}\frac{k}{\mu r_\alpha^2}(\bar{h}' + k\alpha) + M(\tau) \tag{36}$$

As stated, we assume quasi-static aerodynamics with a lift curve slope of 2π.

Here, we will consider that the airfoil is subjected to turbulence in the vertical direction, which we will treat as an external random forcing, that is, an additive white noise (delta correlated) process $W(\tau)$ that corresponds to $L(\tau)$ and $M(\tau)$ in Eqs. (35) and (36). Future work will consider colored noise approximations for the turbulence. The corresponding Itô-type stochastic differential equations are

$$d\bar{h} = y\,d\tau \tag{37}$$

$$dy = -\left(\left[2\xi_h \frac{\omega_h}{\omega_\alpha} + \pi \frac{k}{\mu}\right] y + \left(\frac{\omega_h}{\omega_\alpha}\right)^2 \left(\bar{h} + b^2 \frac{K_h^{nl}}{K_h}\bar{h}^3\right) + \pi \frac{k^2}{\mu}\alpha\right) d\tau + \sigma_L\, dW(\tau) \tag{38}$$

$$d\alpha = z d\tau \tag{39}$$

$$dz = -\left(2\xi_\alpha z + \left[1 - \pi\frac{e}{b}\frac{k^2}{\mu r_\alpha^2}\right]\alpha + \frac{K_\alpha^{nl1}}{K_\alpha}\alpha^3 + \frac{K_\alpha^{nl2}}{K_\alpha}\alpha^5 - \pi\frac{e}{b}\frac{k}{\mu r_\alpha^2}y\right)d\tau + \sigma_M dW(\tau) \tag{40}$$

The Fokker–Planck equation, which is to be solved using DQMOM, is given by

$$\begin{aligned}\frac{\partial f}{\partial \tau} &= -\frac{\partial}{\partial \bar{h}}\{fy\} + \frac{\partial}{\partial y}\left\{f\left[\left(2\xi_h\frac{\omega_h}{\omega_\alpha} + \pi\frac{k}{\mu}\right)y + \left(\frac{\omega_h}{\omega_\alpha}\right)^2\left(\bar{h} + b^2\frac{K_h^{nl}}{K_h}\bar{h}^3\right) + \pi\frac{k^2}{\mu}\alpha\right]\right\} \\ &\quad - \frac{\partial}{\partial \alpha}\{fz\} + \frac{\partial}{\partial z}\left\{f\left[2\xi_\alpha z + \left(1 - \pi\frac{e}{b}\frac{k^2}{\mu r_\alpha^2}\right)\alpha + \frac{K_\alpha^{nl1}}{K_\alpha}\alpha^3 + \frac{K_\alpha^{nl2}}{K_\alpha}\alpha^5 - \pi\frac{e}{b}\frac{k}{\mu r_{\alpha^2}}y\right]\right\} + \frac{1}{2}\frac{\partial^2}{\partial y^2}\{\sigma_L^2 f\} + \frac{1}{2}\frac{\partial^2}{\partial z^2}\{\sigma_M^2 f\}\end{aligned} \tag{41}$$

The following values for the parameters are used in generating the results to follow: $\frac{\omega_h}{\omega_\alpha} = 0.8$, $b = 1.0$, $\xi_\alpha = \xi_h = 0.05$, $x_\alpha = 0.0$, $\mu = 10.0$, $e = 0.1$, $r_\alpha^2 = 0.25$, $\frac{K_h^{nl}}{K_h} = 0.1$, $\frac{K_\alpha^{nl1}}{K_\alpha} = -0.1$, and $\frac{K_\alpha^{nl2}}{K_\alpha} = 0.1$. Also, the ratio $\frac{\sigma_M}{\sigma_L}$ was fixed to be 0.1. For these parameter values, the deterministic system has a subcritical Hopf bifurcation at $k = 1.475$ and a saddle-node bifurcation at $k \approx 1.460$. Figure 18 shows the standard deviation of α and $\bar{h}$ versus σ_L^2 for a value of k below the saddle-node value, $k = 1.30$. The stationary values shown for the DQMOM solution are computed by solving the stationary form of the DQMOM discretization of Eq. (41). Twelve quadrature points are used, giving a total of 60 unknown weight and abscissa values. These unknowns are found by solving the set of 60 nonlinear algebraic equations using a modified Powell hybrid method [30]. The Monte Carlo results shown in Fig. 18 use 100,000 realizations with a time step of 0.00025 for the Euler–Mayurama numerical integration of Eq. (40). Converged statistics for the Monte Carlo simulation took approximately 20 h using an message passing interface based parallel solution with 10 dual-core Pentium 4 Xeon EM64T 3.2 GHz processors. The stationary DQMOM solution, if provided with a reasonable initial guess for the nonlinear solver, took only seconds.

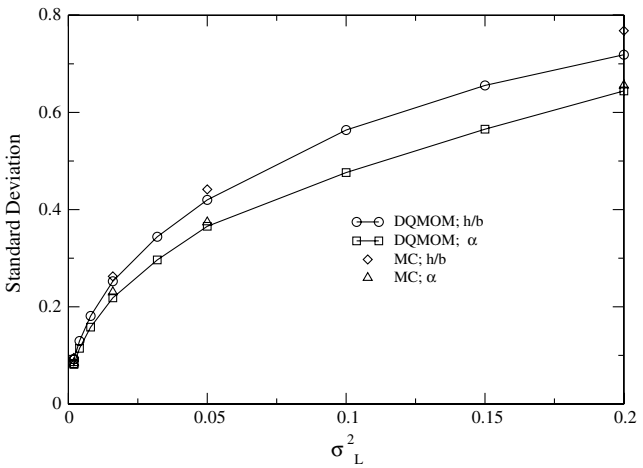

Fig. 18 The normalized plunge degree of freedom and pitch degree of freedom standard deviation vs σ_L^2 for the typical section airfoil with nonlinear structural model; $k = 1.300$.

Future investigation of this problem will include computing the statistics for values of k, which fall in the hysteresis region ($1.460 \geq k < 1.475$) and above the subcritical bifurcation point (linear flutter point) of $k = 1.475$, and studying the effects of multiplicative noise in the problem parameters.

IV. Conclusions

A new method, the DQMOM, is presented for the numerical solution of the Fokker–Planck equations. In DQMOM, the probability density function is written as a summation of products of Dirac delta functions. The location of the quadrature abscissas in probability space (arguments of the delta function) become part of the solution and are obtained (along with the quadrature weights) as solutions of their evolution equations. These evolution equations are obtained using the Fokker–Planck equation using constraints on the generalized moments of the stochastic processes. The use of the Dirac delta function results in a much simpler (over traditional weighted-residual methods) treatment of nonlinear drift and diffusion terms.

In this paper, the method has been used to compute moments for one-, two-, and four-dimensional processes that possess nonlinear stochastic differential equations. In the one-dimensional problem, the stationary moments (second, fourth, and sixth) computed using DQMOM compare well with the analytical solutions. The distribution for this problem is bimodal. The two-dimensional problems were the noisy van der Pol oscillator and a problem which contains, for the deterministic system, both a saddle-node bifurcation and subcritical Hopf bifurcation. For both these examples, stationary second- and fourth-order moments computed using DQMOM compared well with those computed using a Monte Carlo solution of the respective stochastic differential equations. Trends in the normalized moments with respect to additive noise level and the bifurcation parameter are reported for the stochastic saddle-node/subcritical problem for what appears to be the first time. These results could be useful in analyzing similar behavior for aeroelastic systems that contain such stability properties.

Statistics are computed for a typical section airfoil in subsonic flow with nonlinear pitch and plunge stiffness (four-dimensional stochastic process). The airfoil is subjected to delta correlated random forcing that approximates turbulence in the transverse component of flow velocity. The stationary standard deviation results computed with the DQMOM approach for a reduced frequency value below the deterministic saddle point compare well, for both the pitch and plunge degrees of freedom, with those computed using a numerical integration of the stochastic differential equations. Future investigation of this problem will include reduced frequency values within the hysteresis region and above the subcritical bifurcation (flutter) point. Also, the effect of using colored noise approximations for the turbulence will be studied for this particular problem, which contains both a saddle-node and subcritical bifurcation.

Finally it should be stated that, like most new numerical methods, DQMOM has some unresolved issues that require further study. For example, for particular problems and certain sets of constrained moments, the system of implicit, nonlinear differential equations generated with the method can become singular during the time evolution of the equations. A systematic means for choosing moment constraints that do not produce this undesirable effect is currently being sought by the authors.

Appendix: Example of Matrix Equations Resulting from the DQMOM Solution of the Fokker-Planck Equation

Here, the system given in Eq. (17) will be written out for the one-dimensional, nonlinear stochastic process given in Sec. III.A. In this example, four quadrature points will be used with all moments up to and including the seventh moment constrained. For this choice of parameters, the terms in Eq. (17) are as follows:

$$\mathbf{A} = \begin{bmatrix} 1 & 1 & 1 & 1 & 0 & 0 & 0 & 0 \\ 0 & 0 & 0 & 0 & 1 & 1 & 1 & 1 \\ -x_1^2 & -x_2^2 & -x_3^2 & -x_4^2 & 2x_1 & 2x_2 & 2x_3 & 2x_4 \\ -2x_1^3 & -2x_2^3 & -2x_3^3 & -2x_4^3 & 3x_1^2 & 3x_2^2 & 3x_3^2 & 3x_4^2 \\ -3x_1^4 & -3x_2^4 & -3x_3^4 & -3x_4^4 & 4x_1^3 & 4x_2^3 & 4x_3^3 & 4x_4^3 \\ -4x_1^5 & -4x_2^5 & -4x_3^5 & -4x_4^5 & 5x_1^4 & 5x_2^4 & 5x_3^4 & 5x_4^4 \\ -5x_1^6 & -5x_2^6 & -5x_3^6 & -5x_4^6 & 6x_1^5 & 6x_2^5 & 6x_3^5 & 6x_4^5 \\ -6x_1^7 & -6x_2^7 & -6x_3^7 & -6x_4^7 & 7x_1^6 & 7x_2^6 & 7x_3^6 & 7x_4^6 \end{bmatrix}$$

$$\mathbf{z} = \begin{Bmatrix} \frac{\mathrm{d}w_1}{\mathrm{d}t} \\ \frac{\mathrm{d}w_2}{\mathrm{d}t} \\ \frac{\mathrm{d}w_3}{\mathrm{d}t} \\ \frac{\mathrm{d}w_4}{\mathrm{d}t} \\ \frac{\mathrm{d}\mu_1}{\mathrm{d}t} \\ \frac{\mathrm{d}\mu_2}{\mathrm{d}t} \\ \frac{\mathrm{d}\mu_3}{\mathrm{d}t} \\ \frac{\mathrm{d}\mu_4}{\mathrm{d}t} \end{Bmatrix}$$

$$\mathbf{F} = \begin{Bmatrix} 0 \\ \sum_{i=1}^4 w_i [D_1^{(1)}|_{x_i}] \\ \sum_{i=1}^4 w_i [2x_i D_1^{(1)}|_{x_i} + 2D_{11}^{(2)}|_{x_i}] \\ \sum_{i=1}^4 w_i [3x_i^2 D_1^{(1)}|_{x_i} + 6x_i D_{11}^{(2)}|_{x_i}] \\ \sum_{i=1}^4 w_i [4x_i^3 D_1^{(1)}|_{x_i} + 12x_i^2 D_{11}^{(2)}|_{x_i}] \\ \sum_{i=1}^4 w_i [5x_i^4 D_1^{(1)}|_{x_i} + 20x_i^3 D_{11}^{(2)}|_{x_i}] \\ \sum_{i=1}^4 w_i [6x_i^5 D_1^{(1)}|_{x_i} + 30x_i^4 D_{11}^{(2)}|_{x_i}] \\ \sum_{i=1}^4 w_i [7x_i^6 D_1^{(1)}|_{x_i} + 42x_i^5 D_{11}^{(2)}|_{x_i}] \end{Bmatrix}$$

where, for the problem in the one-dimensional nonlinear process example, $D_1^{(1)} = x - x^3$ and $D_{11}^{(2)} = \frac{\sigma^2}{2}$.

Acknowledgment

The authors would like to acknowledge the University of Oklahoma Supercomputing Center, which provided supercomputing time to the authors, enabling them to complete this work.

References

[1] Ibrahim, R., Orono, P., and Madaboosi, S., "Stochastic Flutter of a Panel Subjected to Random In-Plane Forces Part I: Two Mode Interaction," *AIAA Journal*, Vol. 28, No. 4, 1990, pp. 694–702. doi:10.2514/3.10448

[2] Ibrahim, R., and Orono, P., "Stochastic Flutter of a Panel Subjected to Random In-Plane Forces. II—Two and Three Mode Non-Gaussian Solutions," AIAA Paper 1990-986, 1990.

[3] Ibrahim, R., Beloiu, D., and Pettit, C., "Influence of Joint Relaxation on Deterministic and Stochastic Panel Flutter," *AIAA Journal*, Vol. 43, No. 7, July 2005, pp. 1444–1454. doi:10.2514/1.7208

[4] Vaicaitis, R., Dowell, E., and Ventres, C., "Nonlinear Panel Response by a Monte Carlo Approach," *AIAA Journal*, Vol. 12, May 1974, pp. 685–691. doi:10.2514/3.49320

[5] Olson, M., "Some Flutter Solutions Using Finite Elements," *AIAA Journal*, Vol. 8, 1970, pp. 747–752. doi:10.2514/3.5751

[6] Pettit, C. L., "Uncertainty Quantification in Aeroelasticity: Recent Results and Research Challenges," *Journal of Aircraft*, Vol. 41, No. 5, Sept.–Oct. 2004, pp. 1217–1229. doi:10.2514/1.3961

[7] Risken, H., *The Fokker–Planck Equation: Methods of Solution and Applications*, 2nd ed., Springer–Verlag, New York, 1996.

[8] Rodríguez, R., and Van Kampen, N., "Systematic Treatment of Fluctuations in a Nonlinear Oscillator," *Physica A: Statistical Mechanics and Its Applications (Amsterdam)*, Vol. 85, No. 2, 1976, pp. 347–362. doi:10.1016/0378-4371(76)90054-6

[9] Weinstein, E. M., and Benaroya, H., "The Van Kampen Expansion for the Fokker–Planck Equation of a Duffing Oscillator," *Journal of Statistical Physics*, Vol. 77, Nos. 3/4, 1994, pp. 667–679. doi:10.1007/BF02179455

[10] Voigtlaender, K., and Risken, H., "Solutions of the Fokker–Planck Equation for a Double-Well Potential in Terms of Matrix Continued Fractions," *Journal of Statistical Physics*, Vol. 40, Nos. 3/4, 1985, pp. 397–429. doi:10.1007/BF01017181

[11] Naess, A., and Hegstad, B., "Response Statistics of Van Der Pol Oscillators Excited by White Noise," *Nonlinear Dynamics*, Vol. 5, 1994, pp. 287–297. doi:10.1007/BF00045338

[12] Kumar, P., and Narayanan, S., "Solution of Fokker–Planck Equation by Finite Element and Finite Difference Methods for Nonlinear Systems," *Sadhana*, Vol. 31, No. 4, 2006, pp. 445–461. doi:10.1007/BF02716786

[13] Harrison, G. W., "Numerical Solution of the Fokker Planck Equation Using Moving Finite Elements," *Numerical Methods for Partial Differential Equations*, Vol. 4, 1988, pp. 219–232. doi:10.1002/num.1690040305

[14] Spencer, B., Jr., and Bergman, L., "On the Numerical Solution of the Fokker–Planck Equation for Nonlinear Stochastic Systems," *Nonlinear Dynamics*, Vol. 4, 1993, pp. 357–372. doi:10.1007/BF00120671

[15] Wojtkiewicz, S., and Bergman, L., "Numerical Solution of High Dimensional Fokker–Planck Equations," American Society of Civil Engineers Paper 2000-167, 2000.

[16] Fox, R., *Computational Models for Turbulent Reacting Flows*, Cambridge Univ. Press, Cambridge, England, U.K., 2003.

[17] Marchisio, D., and Fox, R., "Solution of Population Balance Equations Using the Direct Quadrature Method of Moments," *Journal of Aerosol Science*, Vol. 36, 2005, pp. 43–73. doi:10.1016/j.jaerosci.2004.07.009

[18] Fan, R., Marchisio, D., and Fox, R., "Application of the Direct Quadrature Method of Moments to Polydisperse, Gas–Solid Fluidized Beds," *Powder Technology*, Vol. 139, 2004, pp. 7–20. doi:10.1016/j.powtec.2003.10.005

[19] Vedula, P., and Fox, R. O., "Direct Quadrature Method of Moments for the Boltzmann Equation," *Journal of Statistical Physics* (submitted for publication).

[20] Attar, P. J., and Vedula, P., "Direct Quadrature Method of Moments Solution of the Fokker–Planck Equation," *Journal of Sound and Vibration*, Vol. 317, Nos. 1–2, Oct. 2008, pp. 265–272. doi:10.1016/j.jsv.2008.02.037.

[21] Ibrahim, R., *Parametric Random Vibration*, Wiley, New York, 1985.

[22] Petzold, L. R., "A Description of DASSL: A Differential/Algebraic System Solver," *IMACS Trans. Scientific Computing*, Vol. 1, North-Holland, Amsterdam, 1993, pp. 65–68.

[23] Brenan, K., Campbell, S., and Petzold, L., *Numerical Solution of Initial-Value Problems in Differential-Algebraic Equations*, North Holland, Amsterdam, 1989.

[24] Brown, P. N., Hindmarsh, A. C., and Petzold, L. R., "Consistent Initial Condition Calculation for Differential-Algebraic Systems," *SIAM Journal on Scientific Computing*, Vol. 19, No. 5, Sept. 1998, pp. 1495–1512. doi:10.1137/S1064827595289996

[25] To, C., "A Statistical Non-Linearization Technique in Structural Dynamics," *Journal of Sound and Vibration*, Vol. 160, No. 3, 1993, pp. 543–548. doi:10.1006/jsvi.1993.1044

[26] Strogatz, S. H., *Nonlinear Dynamics and Chaos*, Addison Wesley, Reading, MA, 1998.

[27] Attar, P., Dowell, E., and Tang, D., "Modeling Aerodynamic Nonlinearities for Two Aeroelastic Configurations: Delta Wing and Flapping Flag," AIAA Paper 2003-1402, April 2003.

[28] Lin, Y., and Cai, G., *Probabilistic Structural Dynamics: Advanced Theory and Applications*, McGraw-–Hill, New York, 1995.

[29] Dowell, E., Clark, R., Cox, D., Curtiss, H., Jr., Peters, D. A., Scanlan, R., Simiu, E., Sisto, F., and Strganac, T., *A Modern Course in Aeroelasticity*, 4th ed., Kluwer Academic, Norwell, MA, 2004.

[30] Powell, M., "A Hybrid Method for Nonlinear Equations," *Numerical Methods for Nonlinear Algebraic Equations*, edited by P. Rabinowitz, Gordon and Breach Science, London, 1970, pp. 87–144.

E. Livne
Associate Editor